

Comparative study on standard geometrical structures of cantilever-based MEMS piezoelectric energy harvester over T-shaped cantilever beam for low frequency ambient vibrations

SALEM SAADON^{a, b*}, OTHMAN SIDEK^b

^a School of Electrical and Electronic Engineering, Universiti Sains Malaysia (USM), 14300 Nibong Tebal, Pulau Pinang, Malaysia

^b Collaborative Microelectronic Design Excellence Center (CEDEC), Universiti Sains Malaysia (USM), Engineering Campus 14300 Nibong Tebal, Seberang Perai Selatan, Pulau Pinang, Malaysia

The micro-generators can become an alternative to the battery-based solutions in the future, especially for remote systems. In this paper, we proposed a model and presented the simulation of a MEMS-based energy harvester of three different shapes piezoelectric cantilevers under ambient vibration excitation using the COVENTORWARE2010 approach. The designed T-shaped cantilever-based MEMS energy harvester that operates under ambient excitation frequency of 11 Hz within a base acceleration of 1g produces an output power of 2.4 μ w at 5k Ω load.

(Received July 30, 2013; accepted May 15, 2014)

Keywords: Piezoelectric materials, Piezoelectricity, Shaped cantilever, MEMS

1. Introduction

The requirements to maximize the harvested power within the variation of cantilever dimensions, weight and cost are the main challenge to maintain the power capability at ambient vibration frequencies.

Previously, the rectangular shaped cantilevers were widely used according to their ease of fabrication, while the main disadvantage of such shape of cantilever is that the average strain is very poor.

On the last decade, most researchers are focused on the piezoelectric materials and the operating modes of the harvester rather than the geometrical shapes of the cantilever [1-11]. Saadon and Sidek [12], were proposed a brief literature review on micro scale rectangular cantilevered piezoelectric harvesters, they showed that the power harvested is not enough to be applicable.

Baker et al. [13], were examined the effects of the piezoelectric cantilever geometry on the power density in order to find a geometrical shape alternatives to the popular rectangular shape. Mateu and Moll [14] proposed an analytical comparison between a rectangular shape and triangular shaped piezoelectric cantilever having a large clamped end with a small free end. They were proved mathematically that, a triangular piezoelectric cantilever having a base and height similar to the base and length of a rectangular piezoelectric cantilever can withstand a higher strain as well as maximum deflection for a given boundary conditions of the beam. Roundy et al. [15] discussed that, the strain is uniformly distributed

throughout the trapezoidal cantilever structure than a rectangular cantilever, they stated that, a trapezoidal piezoelectric cantilever can generate more than twice the energy that can be generated by a rectangular piezoelectric cantilever, provided that both cantilevers contains the same volume of PZT.

In this paper a T-shaped unimorph cantilever was designed and simulated in order to provide an optimized power as well as effective strain compared to other geometrical shapes using coventorware approach.

2. Theoretical analysis

2.1 Deflection of the rectangular cantilevers

The structure of a rectangular single-layered or multilayered cantilever with length L , width W , equivalent thickness T , equivalent density ρ , and equivalent Young's modulus E , have been shown in Fig. 2.1.

When a force F is applied at the free end of the rectangular cantilever shown in Fig. (2.1), the differential equation of the cantilever can be expressed as,

$$\frac{\partial^2 z(x)}{\partial x^2} = \frac{F(l-x)}{EI} = \frac{12F(l-x)}{Ewt^3} \quad (2.1)$$

where x , is the distance from the fixed end of the cantilever, and I is the moment of inertia of the cross-sectional area ($I = WT^3/12$).

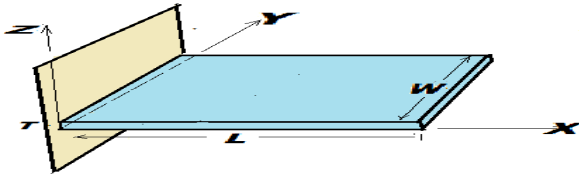


Fig. 2.1. Rectangular shaped cantilever.

The corresponding boundary conditions are:

$$z(0) = 0 \quad (2.2)$$

$$\left. \frac{\partial z(x)}{\partial x} \right|_{x=0} = 0 \quad (2.3)$$

The solution of the differential equation of equations 2.1, 2.2 and 2.3, can be expressed as,

$$z(x) = \frac{2Fx^2(3l-x)}{Ewt^3} = Ax^2(3l-x) \quad (2.4)$$

where A is a constant, $A = 2F/(EWT^3)$.

2.2 Resonance frequency of T-shaped cantilever for low frequency applications

As shown in Fig. 2.2, the function of the width is a piecewise function as,

$$w(x) = \begin{cases} w_0, & x \in [0, l_0] \\ w_1, & x \in [l_0, l_1] \end{cases} \quad (2.5)$$

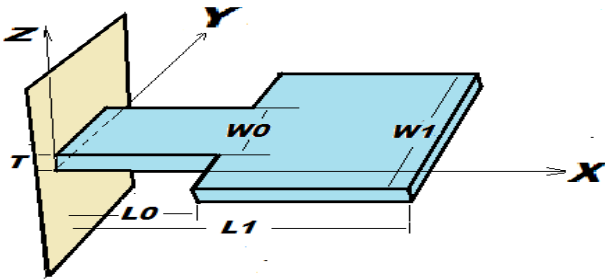


Fig. 2.2. T-shaped cantilever.

In this case, the function $z(x)$ of equation (2.4) can be used as the mode shape, and the displacement at each position of the cantilever can be written as,

$$z(x, t) = Ax^2(3l_1 - x) \sin(2\pi ft + \alpha) \quad (2.6)$$

where, A and α are constants, and t, f are time and frequency respectively.

The kinetic energy can be expressed as,

$$KE = \int_0^{l_1} \frac{1}{2} [\rho t w(x) dx] \left(\frac{\partial z}{\partial t} \right)^2 = 2\pi^2 f^2 A^2 \rho t \cos^2(2\pi ft + \alpha) \int_0^{l_1} w(x) x^4 (3l_1 - x)^2 dx \quad (2.7)$$

Therefore, the maximum kinetic energy of this system is,

$$KE_{\max} = 2\pi^2 f^2 A^2 \rho t \int_0^{l_1} w(x) x^4 (3l_1 - x)^2 dx \quad (2.8)$$

The potential energy can expressed as,

$$V = \int_0^{l_1} \frac{1}{2} EI(x) \left(\frac{\partial^2 z}{\partial x^2} \right)^2 dx = \frac{3}{2} Et^3 A^2 \sin^2(2\pi ft + \alpha) \int_0^{l_1} w(x) (l_1 - x)^2 dx \quad (2.9)$$

where, $I(x) = W(x)T^3/12$, is the moment of inertia of the cross-sectional area.

While the maximum potential energy is,

$$V_{\max} = \frac{3}{2} Et^3 A^2 \int_0^{l_1} w(x) (l_1 - x)^2 dx \quad (2.10)$$

Due to the conservation law of mechanical energy, the maximum of both kinetic and potential energy are equal,

$$KE_{\max} = V_{\max} \quad (2.11)$$

Therefore, from equation (2.11), the resonance frequency of the system can be derived as,

$$f = \sqrt{\frac{(3Et^3/4\pi^2) \int_0^{l_1} w(x) (l_1 - x)^2 dx}{\rho t \int_0^{l_1} w(x) x^4 (3l_1 - x)^2 dx}} \quad (2.12)$$

For the simplicity of the calculations, it is reasonable to define the length ratio as (k), while the width ratio as (r), and both of them are dimensionless and ranged from 0 to 1,

$$r = \frac{w_0}{w_1}, \quad k = \frac{l_0}{l_1} \quad (r \in [0, 1], k \in [0, 1]) \quad (2.13)$$

Therefore, the resonance frequency of equation (2.12) can be rewritten as,

$$f = \frac{10.25t}{2\pi l_1^2} \sqrt{\frac{E}{\rho}} \sqrt{\frac{(r-1)(\frac{1}{3}k^3 - k^2 + k) + \frac{1}{3}}{(r-1)(5k^7 - 35k^6 + 63k^5) + 33}} \quad (2.14)$$

Therefore, the dimensionless characteristic function of the resonance frequency can be defined as,

$$g(r, k) = \sqrt{\frac{(r-1)(\frac{1}{3}k^3 - k^2 + k) + \frac{1}{3}}{(r-1)(5k^7 - 35k^6 + 63k^5) + 33}} \quad (2.15)$$

Thus, the fundamental resonance frequency of the system can be written as,

$$f = \frac{10.25t}{2\pi l_1^2} \sqrt{\frac{E}{\rho}} g(r, k) \quad (2.16)$$

As shown from equation (2.16), the dimensionless characteristic function $g(r, k)$, gives the comparison of different shapes with respect to the normal rectangular shape.

Thus at $W_0=W_1$, the cantilever will have a rectangular shape, and the dimensionless parameter $r=1$, then the dimensionless characteristic function is $g(1, k)$, so the resonance frequency in this case is,

$$f = \frac{10.25t}{2\pi l_1^2} \sqrt{\frac{E}{\rho}} g(r, k) = \frac{1.03t}{2\pi l_1^2} \sqrt{\frac{E}{\rho}} \quad (2.17)$$

The relationship between the resonance frequency and the dimensionless parameters can be shown in Fig. (2.3).

Thus, this cantilever structure can be used for lower frequency applications due to the value of the dimensionless function which is less than 1. In other words, if this T-shape is reversed, i.e the fixed end of the cantilever at the larger width, then the dimensionless function will be greater than 1, so in this case the cantilever can be used at higher frequency applications.

To determine the resonance frequency of a multilayer T-shape cantilever, three variables, such as equivalent density (ρ_{equ}), equivalent young's modulus (E_{equ}) and equivalent thickness (t_{equ}) should be expressed as the following,

$$\rho_{equ} = \frac{\sum_{i=1}^n \rho_i t_i}{\sum_{i=1}^n t_i} \quad (2.18)$$

$$E_{equ} = \frac{\sum_{i=1}^n E_i t_i}{\sum_{i=1}^n t_i} \quad (2.19)$$

$$t_{equ} = \sum_{i=1}^n t_i \quad (2.20)$$

Therefore the fundamental resonant frequency of a n-ltilayered T-shaped piezoelectric cantilever can be expressed in equation (2.21)

$$f = \frac{10.25t_{equ}}{2\pi l_1^2} \sqrt{\frac{E_{equ}}{\rho_{equ}}} g(r, k) \quad (2.21)$$

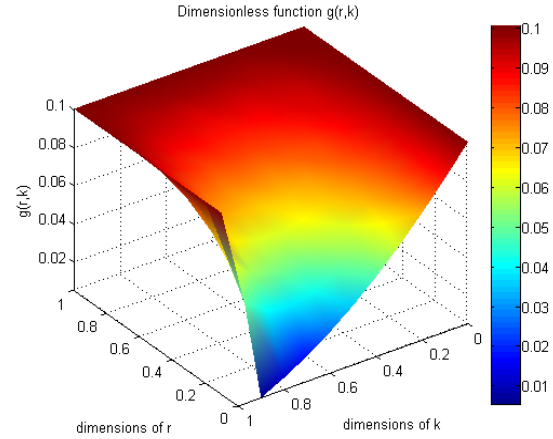


Fig. 2.3. Dimensionless characteristic function.

The affect of the dimensionless function $g(r, k)$ on the resonant frequency of the cantilever can be shown in Fig. 2.3, by using MATLAB.

3. Design and fabrication of T-shaped cantilever beam

The fabrication process setup and layer masks should be carefully edited by using COVENTORWARE approach to produce a solid model of the composite cantilever beam.

3.1 Materials setup

The materials used to achieve this design are Silicon_100 and PZT (lead zirconate titanate), the lower two layers are of Silicon (proof mass + Support layer), while the upper top layer is of PZT material, the specific properties of such material are listed on Table 3.1.

Table 3.1. Material properties of E-shaped piezoelectric cantilever.

Materials	Density (kg/ μm^3)	Modulus of Elasticity (MPa)	Poisson's ratio
PZT	7.55e-15	8.9e+4	0.25
Silicon	2.5e-15	1.69e+5	0.3

3.2 Modeling processes

The masks are shown on the process editor window, all thicknesses of the layers are edited sequentially according to their location at the proposed design of the harvester from down to up.

The process name can be directly selected from the left side menu of the process editor as shown in Fig. 3.1.

Process Editor - [C:/Coventor/Design_Files/Energy/harvester/Devices/PZT-new.proc]

File Edit View Tools Windows Help

Number	Step Name	Layer Name	Material Name	Thickness	Mask Name	Photoresist	Depth	Mask Offset	Sidewall Angle	Comments
0	Substrate	Substrate	SILICON	40	GND					
1	Stack Material	Sacrifice	BPSG	30						
2	Straight Cut				anchor	-	0	0		
3	Conformal Shell	SupportLayer	SILICON	2.5						
4	Straight Cut				SupportLayer	+	0	0		
5	Conformal Shell	Piezo	PZT	2						
6	Straight Cut				Piezo	+	0	0		
7	Stack Material	Proofmass	SILICON	100						
8	Straight Cut				mass	+	0	0		
9	Delete		BPSG							

Fig. 3.1. Process editor and fabrication steps.

3.3 Two-dimensional design creation

By using the same fabrication steps as illustrated in the process editor window at Fig. 3.1, we designed three cantilevers (rectangular, trapezoidal, and T-shaped) to verify the analysis calculations mentioned previously and to show the optimization effect between them, Fig. 3.2 (a, b, and c) shown the 2-dimensional design of these three cantilevers.

All dimensions are in microns, and both cantilevers having same thickness, length, and proof mass volume.

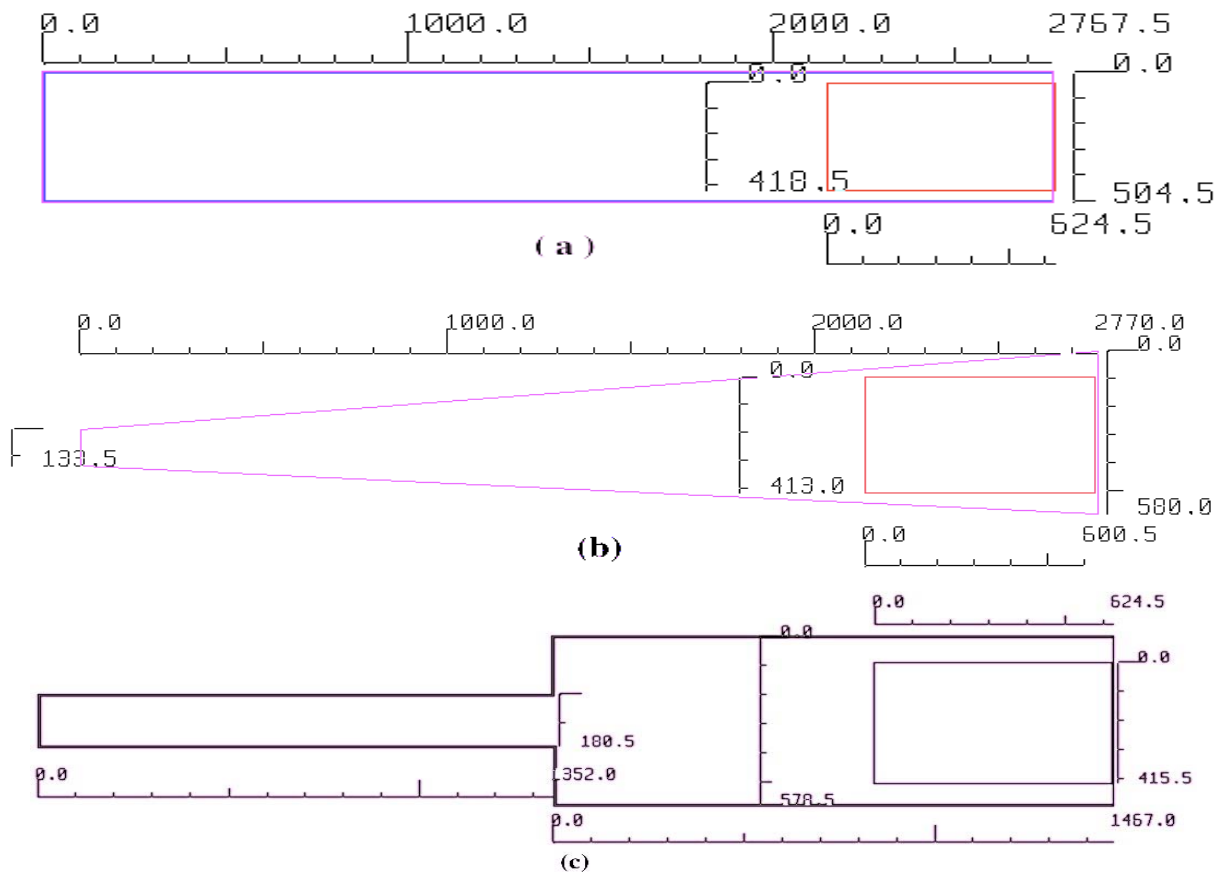


Fig. 3.2. (a) Rectangular beam, (b) Trapezoidal beam, and (c) T-shaped beam.

3.4 Three-dimensional solid model

The three dimensions design of the harvester in the processor window illustrated on Fig. 3.1.

Since all thicknesses are in micron, the Z-scale was enlarged by 2 times to be clearly shown by the readers.

For finite element meshing, the Manhattan mesh type had been used with parabolic element order and element size of 50 to all coordinates.

The solid 3-D model of the three different geometrical shapes shown in Fig. 3.3.

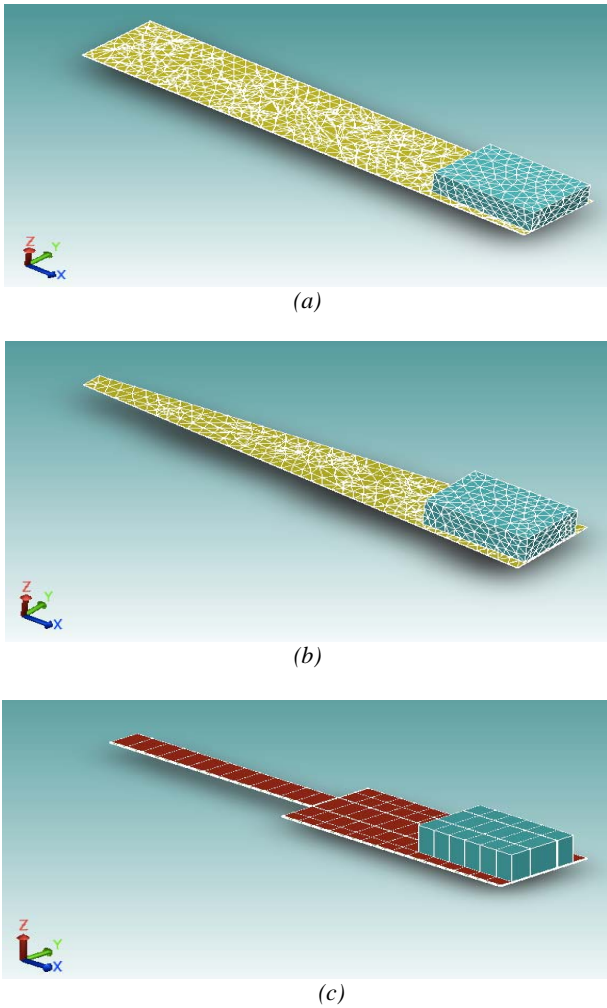


Fig. 3.3. Solid model and Finite Element mesh of: (a) Rectangular, (b) Trapezoidal, and (c) T-shaped beam.

4. Simulation results

4.1 Resonant frequency and harmonic displacement

The geometrical variation of the cantilever beam will control the beam displacement and adjust the desired resonant frequency of the beam accordingly with the environment acceleration and frequency surrounding the piezoelectric harvester at a fixed proof mass volume attached to the beam free end under gravitational acceleration 1 g (9.81 m/s^2).

Variation of the cantilever surface area is the main parameter that can directly affect the displacement and the resonant frequency within the same proof mass.

From the simulation by using Analyzer tap of the coventorware 2010, the three different shaped cantilevers, that were rectangular, trapezoidal and T-shaped cantilever are simulated and resulted in three different frequencies at their maximum tip deflection, 62 Hz, 18 Hz, and 11 Hz respectively.

As shown in Fig. 3.4 (a,b, and c), the lowest frequency can be achieved by using the T-shaped cantilever, which is the main objective of this study.

The strain distribution density on the cantilever urface area will be varied accordingly with the geometrical surface area of the piezoelectric cantilever.

The narrow width clamped end of the cantilever will generate a high stress at that end of the cantilever compared to the free end stress density.

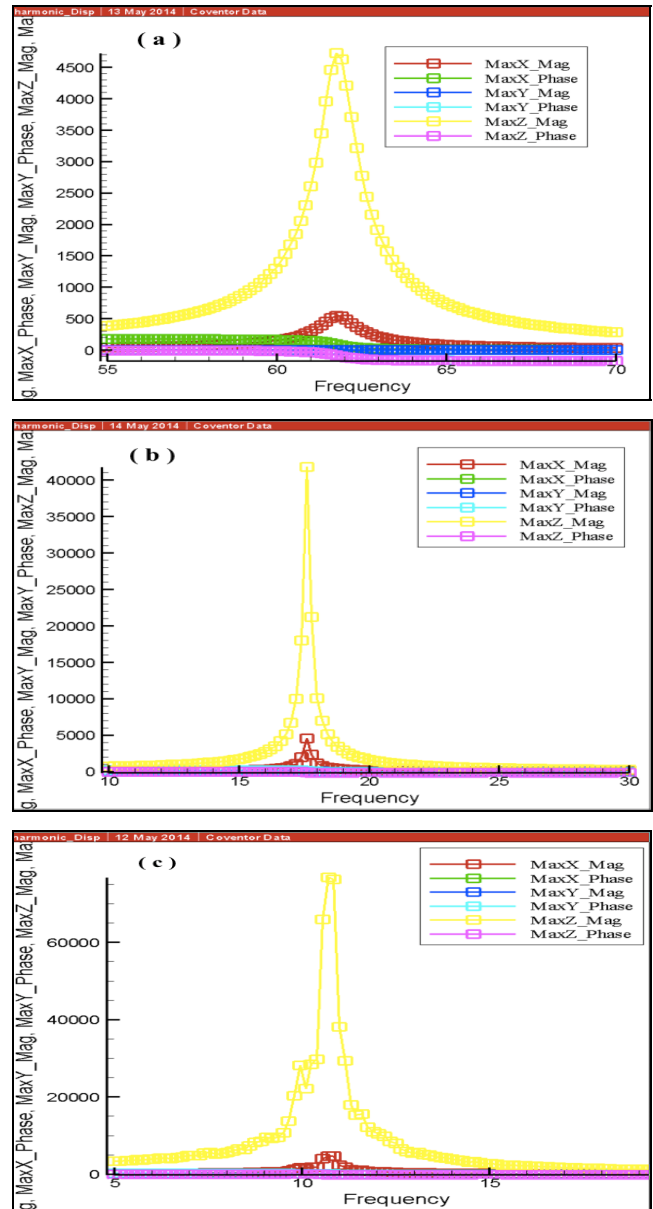


Fig. 3.4. Resonant frequency response and beam displacement: (a) Rectangular (b) Trapezoidal, and (c) T-shaped cantilever beam.

The simulation results obtained by T-shaped piezoelectric cantilever are agree with the analytical equations derived previously.

The reduction function affects on the estimated resonant frequency at the T-shaped cantilever have a good attention to the simulated results.

4.2 Voltage, Current, and Power

A load resistance of $5k\Omega$ was connected across the upper and lower piezoelectric PZT layer surfaces of each cantilever to maintain the output generated power.

All output voltages, currents and powers are listed in Table 4.1, indicated that a maximum power, current, and voltage can be generated across the T-shaped cantilever at lower frequency of 11 Hz than those of trapezoidal cantilever, while lower power and voltage can be generated at the piezoelectric surfaces of the trapezoidal cantilever, since its generated voltage is slightly more than that generated by the rectangular shape but less than the voltage that generated by the T-shaped cantilever.

However, the the current generated by the T-shaped cantilever is higher than that generated by the rectangular shaped cantilever but equal to that generated by the trapezoidal cantilever.

Thus, the piezoelectric energy harvester performance can be enhanced by using T-shaped cantilever instead of the standard shaped cantilevers especially on low frequency ambient vibrations.

Table 4.1. Output voltage, current, and power of the beam.

Cantilever shape	Voltage (V)	Current (μA)	Power (μw)
Rectangular	0.1	19	1.9
Trapezoidal	0.11	20.2	2.3
T-Shaped	0.12	20.2	2.4

The output delivered power by the existing cantilevers were shown graphically in Fig. 4.1

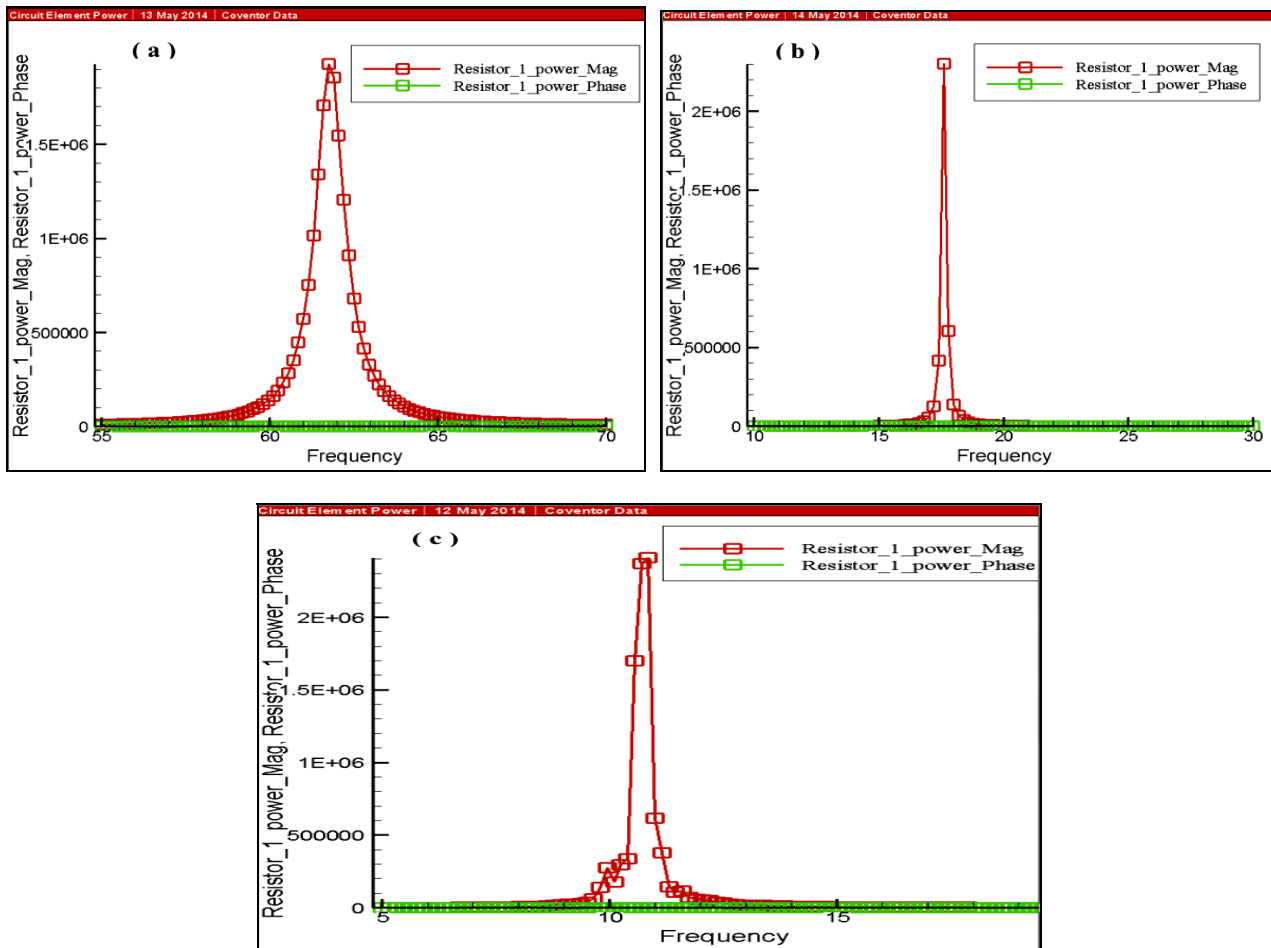


Fig. 4.1. Output harvested power: (a) Rectangular, (b) Trapezoidal, and (c) T-shaped cantilever.

5. Conclusions

The Analyzer/MemMech model predicts that the maximum obtained output voltage, current, and power was fluctuate depending on the geometrical surface structure of the cantilever where the strain distributed having an affect, whereas at low frequency applications, the T-shaped

cantilever is more applicable than the trapezoidal and rectangular shape cantilevers.

The micro fabrication process is approximately the same during all simulation steps, in the open circuit limit, the limit that actually simulated using TiePotential Surface BC. This reported output voltage from the Analyzer/MemMech simulation is about 0.1, 0.11, and 0.12 V across rectangular, trapezoidal, and T-shaped

cantilevers respectively, which gives an agree results compared to previous researchers using MEMS scale simulations.

The power through the 5K Ohms is the more important in this paper, since the maximum power is produced at the loads below the open circuit limits, the base acceleration amplitude will affect the power limitations of the harvester. In the case of T-shaped cantilever, the Analyzer/MemMech prediction is 2.4 microwatts across the load of 5 kilo-ohms compared to the delivered output power of the other standard cantilevers of the same thickness and materials.

Acknowledgements

This work is supported by Universiti Sains Malaysia (USM) fellowship, the Postgraduate Research Grant Scheme PRGS (1001/PELECT/8044039) and Research University Grant RU Grant (1001/PCEDEC/854003).

References

- [1] M. Marzencki, S. Basrour, B. Charlot, A. Grasso, M. Colin, L. Valbin, DTIP'05, Montreux, Switzerland; 2005.
- [2] M. Marzencki, Y. Ammar, S. Basrour, *Sensors Actuat A – Phys.* **145**, 363 (2008).
- [3] D. Shen, J. H. Park, J. Ajitsaria, S. Y. Choe, H. C. Wikle, D. J. Kim, *J Micromech Microeng*; 18 (2008).
- [4] M. Renaud, K. Karakaya, T. Sterken, P. Fiorini, C. Van Hoof, R. Puers, *Sensors Actuat A – Phys.* **145**, 380-6 (2008).
- [5] H. B. Fang, J. Q. Liu, Z. Y. Xu, L. Dong, L. Wang, D. Chen, et al. *Microelectron J*, **37**, 1280-4 (2006).
- [6] J. Q. Liu, H. B. Fang, Z. Y. Xu, X. H. Mao, X. C. Shen, D. Chen, et al. *Microelectron J*, **39**, 802-6 (2008).
- [7] Y. B. Jeon, R. Sood, J. H. Jeong, S. G. Kim, *Sensors Actuat A – Phys.* **122**, 16-22 (2005).
- [8] B. S. Lee, W. J. Wu, W. P. Shih, D. Vasic, F. Costa, In: 2007 IEEE ultrasonics symposium proceedings, **1-6**, 1598 (2007).
- [9] B. S. Lee, S. C. Lin, W. J. Wu, X. Y. Wang, P. Z. Chang, C. K. Lee, *J Micromech Microeng*. 19 (2009).
- [10] P. Muralt, M. Marzencki, B. Belgacem, F. Calame, S. Basrour, *Procedia Chem.* **1**, 1191-4 (2009).
- [11] R. Elfrink, T. M. Kamel, M. Goedbloed, S. Matova, D. Hohlfeld, Y. van Anandel, et al. *J Micromech Microeng.* **19**, (2009).
- [12] S. Saadon, O. Sidek, *Energy Conversion and Management* **52**, 500 (2011).
- [13] L. Mateu, F. Moll, *J Intell Mater Syst Struct.* **16**, 835 (2005).
- [14] S. Roundy, E. S. Leland, J. Baker, E. Carleton, E. Reilly, E. Lai, et al. *IEEE Pervasive Comput.* **4**, 28 (2005).
- [15] J. Baker, S. Roundy, P. Wright, In: Proceeding 3rd international energy conversion engineering conference, San Francisco, California; August 15-18, 2005.
- [16] James M. Gere, Stephen P. Timoshenko, *Mechanics of materials*. 2nd. (1984), Belmont, Ca: Brooks/Cole Engineering.
- [17] Yi, Jeong Woo, Shih, Wan Y. Shih, Wei-Heng, *Journal of Applied Physics*, **91**(3),1680 (2002).
- [18] J. E. Sader, I. Jarson, M. Paul, L. R. White, *Rev. Sci. Instrum.* **66**, 3789 (1995).

*Corresponding author: saadonsalem@yahoo.com